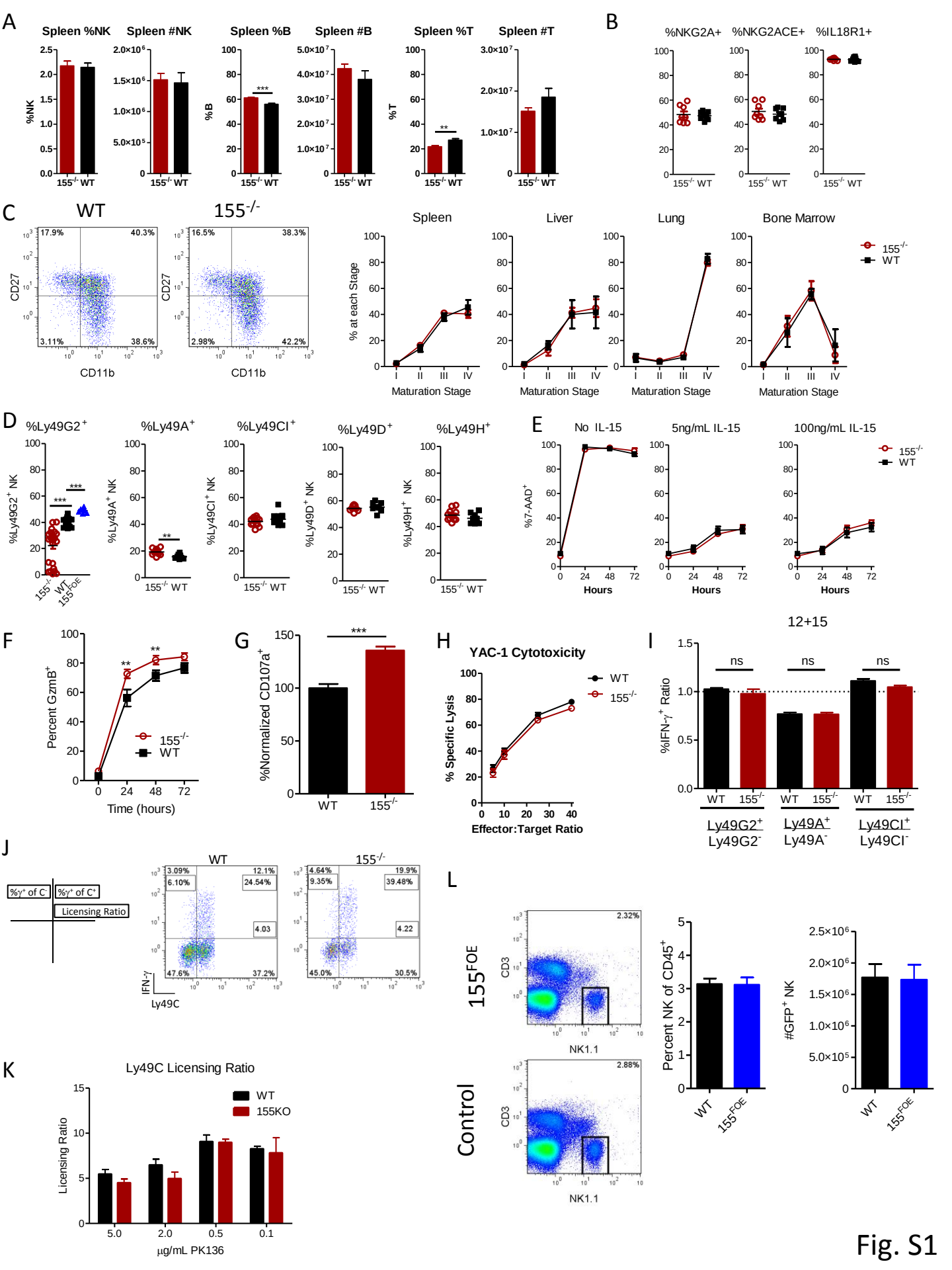
A
Spleen %NK
Spleen #NK
Spleen %B
Spleen #B
Spleen %T
Spleen #T
%NK
%B
%T
155-/- WT
B
%NKG2A+
%NKG2ACE+
%IL18R1+
C
WT
155-/-
17.9%
40.3%
3.11%
38.6%
16.5%
38.3%
2.98%
42.2%
CD27
CD11b
Spleen
Liver
Lung
Bone Marrow
% at each Stage
Maturation Stage
D
%Ly49G2+
%Ly49A+
%Ly49CI+
%Ly49D+
%Ly49H+
%Ly49G2+ NK
%Ly49A+ NK
%Ly49CI+ NK
%Ly49D+ NK
%Ly49H+ NK
155-/- WT 155FOE
E
No IL-15
5ng/mL IL-15
100ng/mL IL-15
%7-AAD+
Hours
F
Percent GzmB+
Time (hours)
G
%Normalized CD107a+
H
YAC-1 Cytotoxicity
% Specific Lysis
Effector:Target Ratio
I
12+15
%IFN-γ+ Ratio
ns
Ly49G2+ Ly49G2-
Ly49A+ Ly49A-
Ly49CI+ Ly49CI-
J
%γ+ of C-
%γ+ of C+
Licensing Ratio
IFN-γ
Ly49C
K
Ly49C Licensing Ratio
Licensing Ratio
µg/mL PK136
WT
155KO
L
155FOE
Control
CD3
NK1.1
2.32%
2.88%
Percent NK of CD45+
#GFP+ NK

Fig. S1

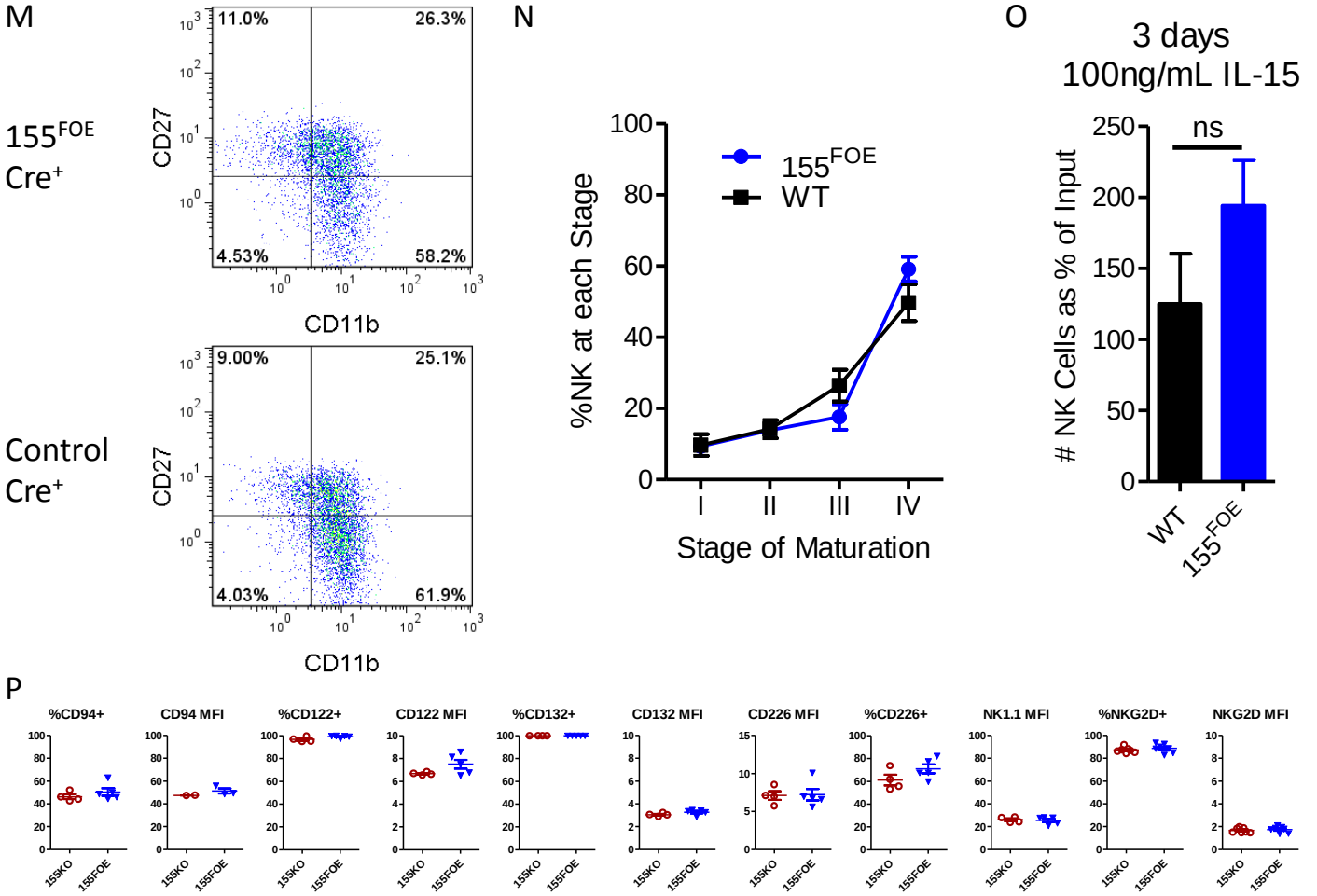

Supplemental Figure 1. miR-155$^{-/-}$ and 155^{FOE} mice have an intact NK cell compartment at baseline. (A) The lymphocyte compartment of miR-155$^{-/-}$ mice demonstrates slight alterations in B and T cell percentages, but no significant differences in absolute number, and no alterations in NK cell percentage or number. N=8-12 mice per group, from 3 independent experiments. **(B)** NK cells from miR-155$^{-/-}$ mice exhibit similar expression of NKG2A, combined NKG2C,A,E, and IL-18R1 compared to WT controls. **(C)** NK cells from miR-155$^{-/-}$ mice exhibit normal maturation in the spleen, liver, bone marrow and lung, compared to littermate controls as defined by CD27 and CD11b. Stage 1: CD27^{-}CD11b^{-}, Stage 2 CD27^{+}CD11b^{-}, stage 3: CD27^{+}CD11b^{+}, stage 4: CD27^{-}CD11b^{+}. Shown are representative spleens (top) and summary data (bottom) from N=7-10 mice per group from at least 3 independent experiments. **(D)** The NK cell Ly49 repertoire is slightly altered in miR-155$^{-/-}$ and 155^{FOE} mice, with miR-155$^{-/-}$ NK cells exhibiting significantly decreased Ly49G2 and modestly increased Ly49A percentages, and 155^{FOE} NK cells exhibiting increased Ly49G2 percentages. Ly49C/I, Ly49D, and Ly49H expression are similar in NK cells from miR-155$^{-/-}$ and control mice. Of note, the ligands for Ly49G2 are not present in C57Bl/6 mice, and are thus unlikely to affect NK cell responses in this genetic model. Neither Ly49G2 or Ly49A are direct targets of miR-155. N=8-28 mice per group, from 2-8 independent experiments. **(E)** NK cells from miR-155$^{-/-}$ mice exhibit no difference in survival, as measured by 7-AAD positivity, after IL-15 culture, compared to WT controls, after culture in cRPMI without IL-15, with 5ng/mL rmIL-15, or 100ng/mL rmIL-15 for 24, 48, or 72 hours. N=6 mice per group from 2-3 independent experiments. **(F)** NK cells from WT or miR-155$^{-/-}$ mice were cultured in rmIL-15 for 24, 48, or 72 hours and assayed for intracellular granzyme B expression by flow cytometry. A significantly higher proportion of miR-155$^{-/-}$ NK cells were positive for GzmB protein following activation. Data shown are mean ± SEM percent GzmB positive NK cells, and summarize at least 8 mice per group from 3 independent experiments. **(G)** miR-155$^{-/-}$ NK cells also had increased degranulation (surface CD107a) after activating NK receptor ligation (anti-NK1.1). NK cells were cultured for 6 hours with plate-bound α-NK1.1, and then assayed for cell surface CD107a by flow cytometry as a surrogate of degranulation. These data are mean ± SEM normalized CD107a^{+} NK cells from at least 12 mice per group from 4 independent experiments. **(H)** NK cells from miR-155$^{-/-}$ mice do not display enhanced killing. **(I)** Ly49G2 and Ly49A expression does not determine IFN-γ responsiveness in 155$^{-/-}$ NK cells. **(J-K)** No differences in licensing were detected between 155$^{-/-}$ and WT NK cells. Licensing ratio is indicated in lower part of upper right quadrant. (**L**) NK cell percentages and numbers are equivalent in the spleens of miR-155^{FOE} and WT mice. Left: Representative flow plots. Middle: Summary data showing the percentage of NK cells is the same in miR-155^{FOE} and WT mice. Right: Summary data showing the absolute number of NK cells in the spleen is the same in miR-155^{FOE} and WT mice. (**M**) Representative bivariate flow plots showing similar NK cell maturation as defined by CD27 and CD11b in miR-155^{FOE} and WT mice. (**N**) Summary data showing similar NK cell maturation (mean + SEM percentage of each stage) in miR-155^{FOE} and WT mice. N=2-4 mice per group from 2-3 independent experiments. (**O**) # of NK cells after culture for 3 days in 100ng/mL IL-15, normalized to input. N = 3 groups of mice from 2 independent experiments. (**P**) Further surface phenotyping of resting miR-155KO and miR-155FOE NK cells. N = 4-5 mice per genotype from 2 independent experiments.

Fig. S1

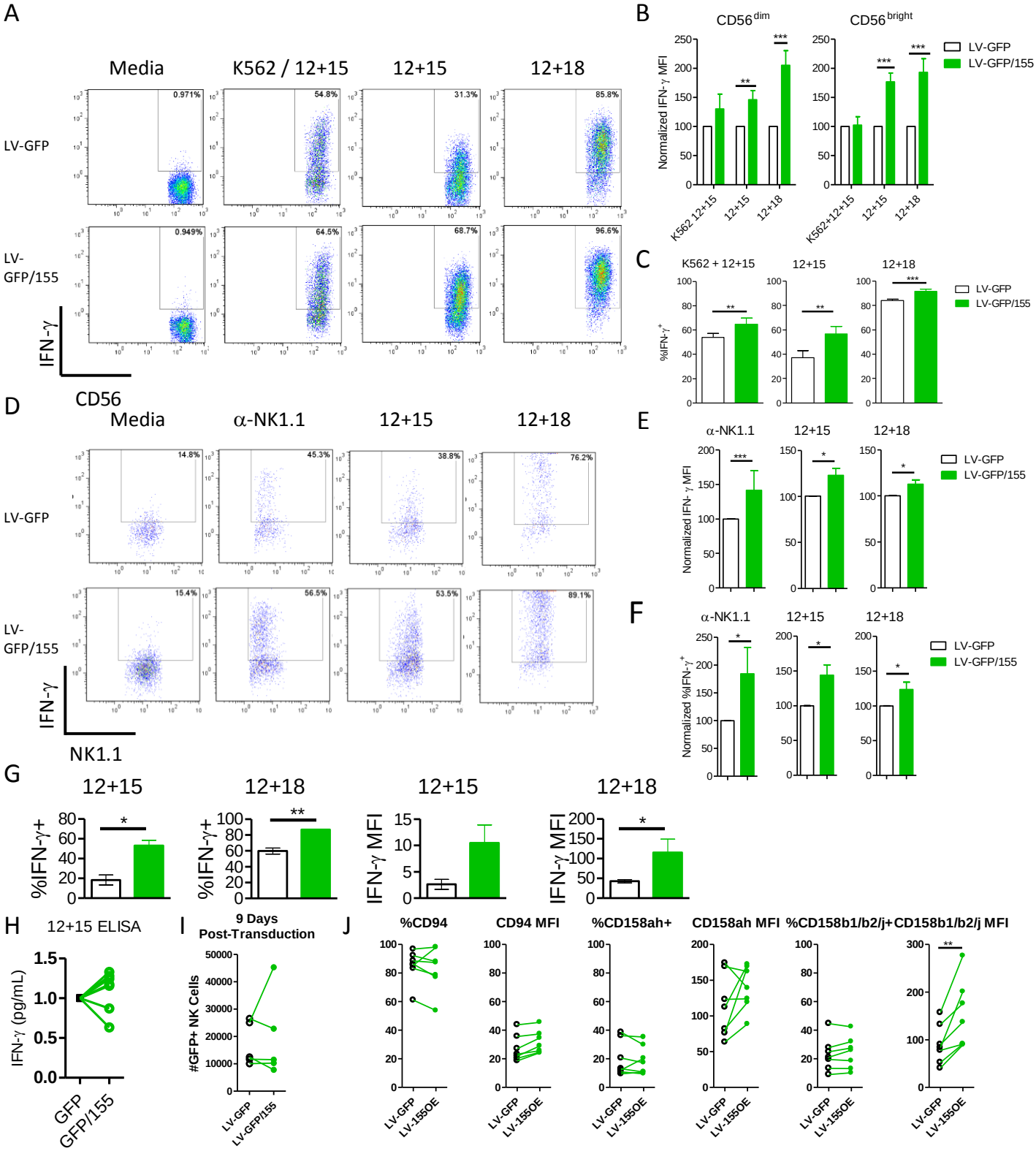

Supplemental Figure 2. LV-GFP/155 transduced human and mouse NK cells produce more IFN-γ due to increased IFN-γ⁺ percentages *and* increased IFN-γ MFI. Human **(A-C)** and mouse **(D-F)**) NK cells were transduced as in (Fig. 2), and then analyzed by flow cytometry for IFN-γ production. Shown is a representative donor for human transduction, stimulated with media only, K562 / 12+15, 12+15, or 12+18 **(A)**, and summarized MFI **(B)** and %IFN-γ⁺ **(C)**. Similarly, a representative mouse sample is shown, in which NK cells were transduced, GFP⁺ NK cells were sorted, and stimulated with plate bound α-NK1.1, 12+15, or 12+18 **(D)**, with summarized MFI **(E)** and %IFN-γ⁺ **(F)**. Data in (A-C) are representative of 8-10 donors from 4 independent experiments. Data in (D-F) are representative of 4-6 pools of 2-4 mice each from 4-6 independent experiments. **(G)** Human NK cells transduced similarly to (A-C), but stimulated 4 days after culture. Data are from 5 donors in 2 independent experiments. **(H)** Data from Fig. 2 12+15, normalized to each donor. **(I)** Number of cells obtained 9 days after transduction with the indicated viruses. **(J)** Surface repertoire analysis of transduced NK cells from 7 donors in 3 independent experiments.

Fig. S2

A

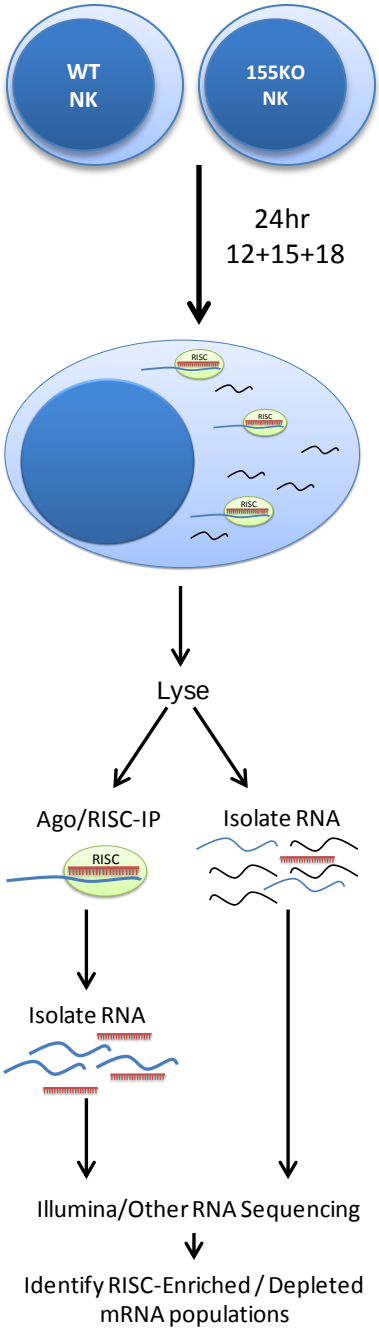

B

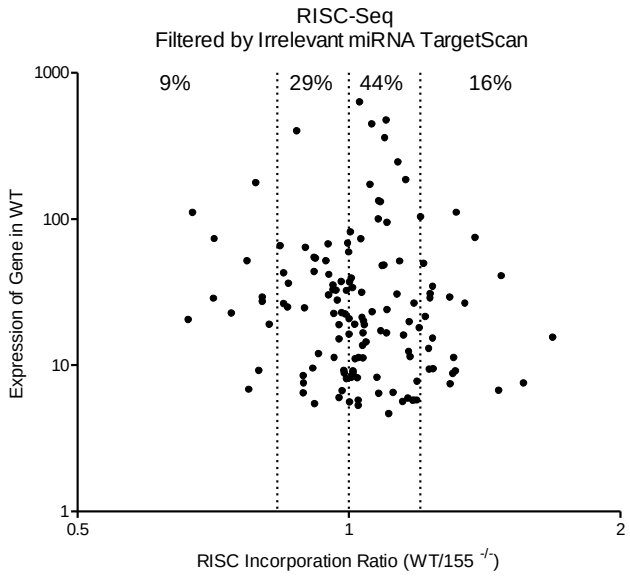

C

	Unfiltered %	miR-15/16 Filtered %	Fold Change
Group 1	18	16	0.88
Group 2	43	44	1.02
Group 3	28	29	1.03
Group 4	11	9	0.81

D

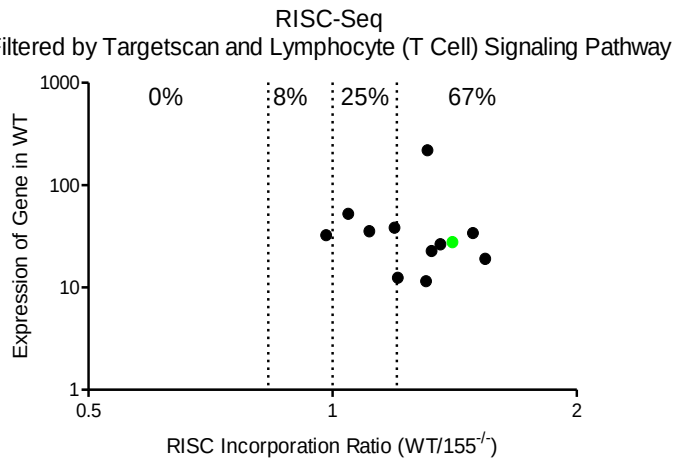

Supplemental Figure 3. Supplemental data for RISC-Seq. (A) Schematic of RISC-Seq, a technique used to identify NK-specific miR-155 targets. First, sorted NK cells are lysed, and separated into two fractions: 1) The RISC-IP fraction, which is immunoprecipitated using anti-Ago2 antibodies, and 2) the total RNA fraction. RNA from both fractions is isolated using Trizol, and then sequenced using an Illumina RNA-seq pipeline. The sequences are aligned to the transcriptome, and mRNAs enriched in the RISC are identified. **(B)** When filtered using TargetScan results for an irrelevant miRNA, no enrichment is observed of the Group 1 (>1.2 RISC Incorporation Ratio) transcripts. **(C)** Quantification of the fold change of the graph in (B). **(D)** The targets in the Lymphocyte (T Cell) Signaling Pathway that exist in our data set are highly enriched in the increased RISC Incorporation Ratio fraction of transcripts.

Fig. S3

A

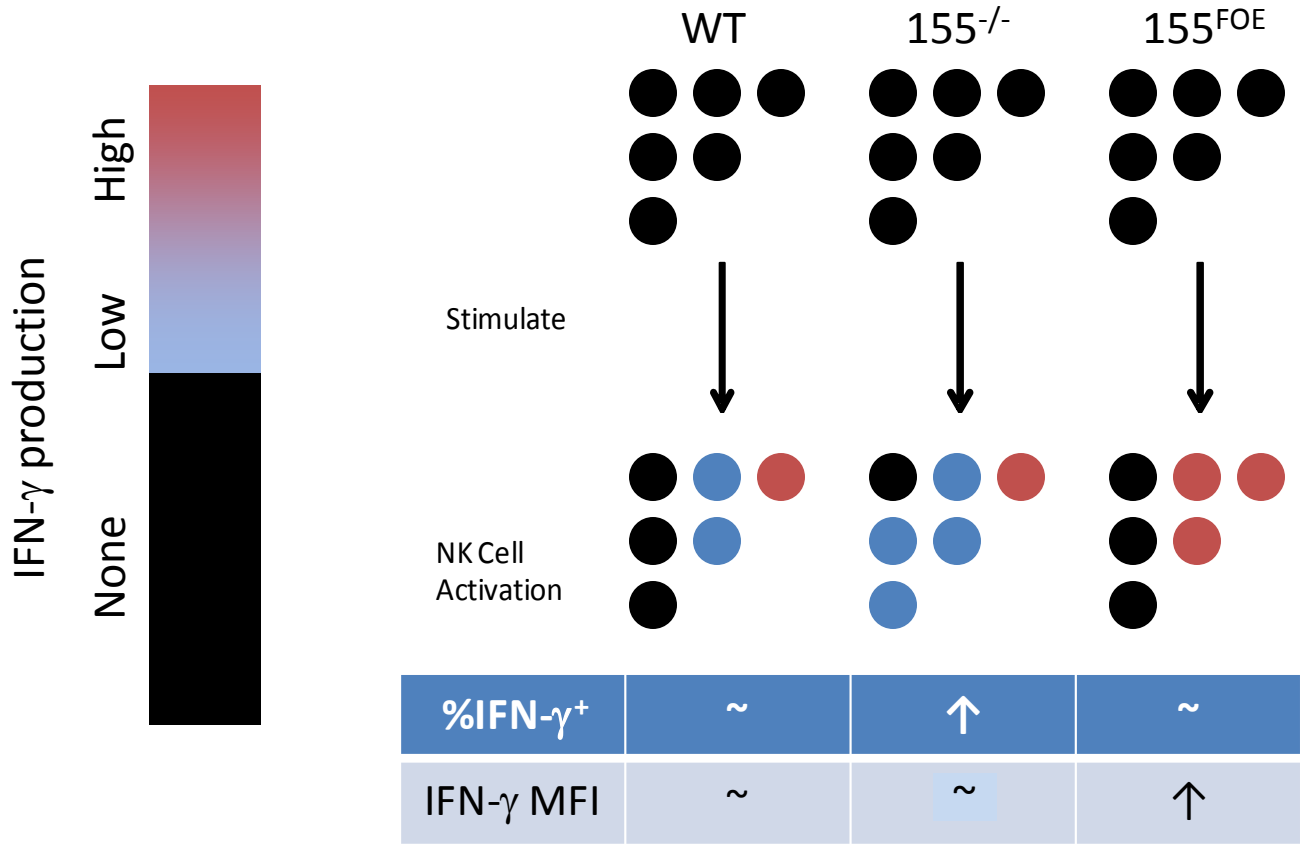

Supplemental Figure 4. Model for miR-155's role in NK cells. **(A)** A summary of the effects of miR-155 alterations on a population of stimulated NK cells. Black = unactivated, blue = activated with low IFN-γ production, red = activated with high IFN-γ production.

Fig. S4